

1
2
3
4
5
6
7
8
9
10
11
12
13
14
15
16
17
18
19
20
21
22
23
24
25
26
27
28
29

Optical properties and bioavailability of dissolved organic matter along a flow-path continuum from soil pore waters to the Kolyma River mainstem, East Siberia

Karen E. Frey^{1,*}, William V. Sobczak², Paul J. Mann³, R. Max Holmes⁴

¹*Graduate School of Geography, Clark University, Worcester, Massachusetts 01610 USA*

²*Department of Biology, College of the Holy Cross, Worcester, Massachusetts 01610 USA*

³*Department of Geography, Northumbria University, Newcastle upon Tyne NE1 8ST UK*

⁴*Woods Hole Research Center, Falmouth, Massachusetts 02540 USA*

*Corresponding author: kfrey@clarku.edu; Tel: 1.508.793.7209

Keywords: East Siberia, Kolyma River, permafrost, DOC, CDOM, biolability

30 **Abstract**

31 The Kolyma River in Northeast Siberia is among the six largest arctic rivers and drains a region
32 underlain by vast deposits of Holocene-aged peat and Pleistocene-aged loess known as yedoma,
33 most of which is currently stored in ice-rich permafrost throughout the region. These peat and
34 yedoma deposits are important sources of dissolved organic matter (DOM) to inland waters that
35 in turn play a significant role in the transport and ultimate remineralization of organic carbon to
36 CO₂ and CH₄ along the terrestrial flow-path continuum. The turnover and fate of terrigenous
37 DOM during offshore transport largely depends upon the composition and amount of carbon
38 released to inland and coastal waters. Here, we measured the ultraviolet-visible optical
39 properties of chromophoric DOM (CDOM) from a geographically extensive collection of waters
40 spanning soil pore waters, streams, rivers, and the Kolyma River mainstem throughout a ~250
41 km transect of the northern Kolyma River basin. During the period of study, CDOM absorption
42 coefficients were found to be robust proxies for the concentration of DOM, whereas additional
43 CDOM parameters such as spectral slopes (*S*) were found to be useful indicators of DOM quality
44 along the flow-path. In particular, the spectral slope ratio (*S_R*) of CDOM demonstrated
45 statistically significant differences between all four water types and tracked changes in the
46 concentration of bioavailable DOC, suggesting that this parameter may be suitable for clearly
47 discriminating shifts in organic matter characteristics among water types along the full flow-path
48 continuum across this landscape. However, despite our observations of downstream shifts in
49 DOM composition, we found a relatively constant proportion of DOC that was bioavailable (~3–
50 6% of total DOC) regardless of relative water residence time along the flow-path. This may be a
51 consequence of two potential scenarios allowing for continual processing of organic material
52 within the system, namely: (a) aquatic microorganisms are acclimating to a downstream shift in

53 DOM composition; and/or (b) photodegradation is continually generating labile DOM for
54 continued microbial processing of DOM along the flow-path continuum. Without such
55 processes, we would otherwise expect to see a declining fraction of bioavailable DOC
56 downstream with increasing residence time of water in the system. With ongoing and future
57 permafrost degradation, peat and yedoma deposits throughout the Northeast Siberian region will
58 become more hydrologically active, providing greater amounts of DOM to fluvial networks and
59 ultimately to the Arctic Ocean. The ability to rapidly and comprehensively monitor shifts in the
60 quantity and quality of DOM across the landscape is therefore critical for understanding potential
61 future feedbacks within the arctic carbon cycle.

62

63 **1. Introduction**

64 There is increasing evidence that inland freshwater ecosystems play a significant role in
65 the global carbon cycle owing to the metabolism of terrestrially-derived organic matter as it
66 moves through fluvial networks from land to ocean (Cole et al., 2007; Battin et al., 2009a, b).
67 Recent research suggests that arctic watersheds may increasingly augment the role of freshwater
68 ecosystems in the global flux of terrestrial carbon to the atmosphere (Walter et al., 2007; Denfeld
69 et al., 2013; Vonk et al., 2013; Hayes et al., 2014; Spencer et al., 2015) and ocean (Frey and
70 Smith, 2005; Frey and McClelland, 2009; Schreiner et al., 2014; Tesi et al., 2014) as a result of
71 climate warming and changing regional hydrology. Terrestrial sources of organic matter
72 generally dominate the energy and carbon fluxes through stream, riverine, and estuarine
73 ecosystems (Mulholland, 1997; Holmes et al., 2008), but the lability and composition of this
74 carbon remain poorly characterized. Headwater and intermediate streams dominate overall
75 channel length in large dendritic drainage basins (e.g., Denfeld et al., 2013), thus the functional

76 role of streams and intermediate rivers is magnified when assessing landscape controls on carbon
77 and nutrient fluxes to the atmosphere and Arctic Ocean.

78 Following the publication of the “river continuum concept” (Vannote et al., 1980), there
79 has been much research focused on the delivery and processing of terrestrially-derived organic
80 matter within temperate stream ecosystems. Through these studies, it has been shown that
81 biological processes within streams alter the transport of organic matter to downstream
82 ecosystems (e.g., Webster and Meyer, 1997), but the fate of terrestrial organic matter in arctic
83 streams and rivers has only more recently been explored (e.g., Frey and Smith, 2005; Neff et al.,
84 2006; Holmes et al., 2008; Denfeld et al., 2013; Spencer et al., 2015). Furthermore, a variety of
85 conceptual and pragmatic issues complicate the study of arctic rivers, including: (i) large
86 seasonal variations in discharge accompanied by large seasonal variations in nutrient and organic
87 matter inputs from rivers to the coastal ocean (e.g., McClelland et al., 2012); (ii) the
88 heterogeneity of vegetation, permafrost extent, topography, and soil attributes within arctic
89 watersheds (e.g., Frey and McClelland, 2009); and (iii) spatial and temporal inaccessibility
90 hindering comprehensive sampling; among others.

91 Hydrologic flow-paths and organic matter transport in arctic regions dominated by
92 permafrost are markedly different than temperate regions with well-drained soils. In particular,
93 permafrost-dominated watersheds lack deep groundwater flow-paths owing to the permafrost
94 boundary in soil that prevents deep groundwater movement (Judd and Kling, 2002; Frey et al.,
95 2007). As a result, the delivery of terrestrial-permafrost organic matter to aquatic ecosystems
96 may in fact lack significant terrestrial or groundwater processing. Once dissolved organic matter
97 (DOM) enters aquatic ecosystems, multiple processes remove DOM from the water column: (i)
98 photochemical reactions, where DOM is degraded to CO₂ or to compounds bioavailable for

99 bacterial uptake (Moran and Zepp, 1997; Laurion and Mladenov, 2013; Cory et al., 2014); (ii)
100 flocculation of terrestrial DOM resulting in the settling of particulate organic matter
101 (Wachenfeldt et al., 2009); (iii) loss via aggregation of DOM owing to changes in ionic strength
102 when freshwater mixes with sea water (Sholkovitz, 1976); (iv) DOM sorption to particles and
103 sedimentation (Chin et al., 1998); and/or (v) bacterial uptake and utilization of the bioavailable
104 fraction (Bronk, 2002; Karl and Björkman, 2002; Mann et al., 2014; Spencer et al., 2015).
105 Measurements of waters along a hydrologic flow-path may indeed give insight into the
106 characteristics of DOM as it is modified through these various processes along the soil-stream-
107 river continuum.

108 Recent work on the Kolyma River in Northeast Siberia has identified marked variation in
109 annual discharge that is associated with large pulses of organic matter flux to the Arctic Ocean
110 during spring freshet, providing detailed temporal characterization of DOM in the Kolyma River
111 mainstem across the annual hydrograph (e.g., Mann et al., 2012). Furthermore, selective
112 processing and loss of permafrost-derived DOM has been shown to occur via microbial
113 metabolism throughout the Kolyma River basin, as waters move downstream through the fluvial
114 network (Mann et al., 2014; Mann et al., 2015; Spencer et al., 2015). Here, we complement
115 these previous studies by providing extensive spatial characterization of DOM along a flow-path
116 continuum from soil pore waters to the Kolyma River mainstem during mid-summer (July)
117 baseflow. The heterogeneity of environmental characteristics and extensive continuous
118 permafrost of the Kolyma River basin combine to make this a critical region to investigate and
119 monitor. In particular, we measured the ultraviolet-visible absorption spectra (200–800 nm) of
120 chromophoric DOM (CDOM) from a geographically extensive collection of waters throughout a
121 ~250 km transect of the northern Kolyma River basin, including samples of soil pore waters,

122 streams, rivers, and the Kolyma River mainstem. CDOM absorption and spectral slopes
123 (calculated within log-transformed absorption spectra) were used to investigate contrasting water
124 types and were found to be useful indicators of both the concentration and reactivity of DOM.
125 With ongoing permafrost degradation and subsequent release of a long-term storehouse of
126 organic material into the contemporary carbon cycle, the ability to easily and comprehensively
127 monitor the quantity and quality of DOM across the landscape through investigation of its optical
128 properties is becoming critical for understanding the global significance of the arctic carbon
129 cycle. Here, we explore a full suite of CDOM parameters as well as concentrations of dissolved
130 organic carbon (DOC) and bioavailable DOC as they vary across a full flow-path continuum in
131 the Kolyma River basin in Northeast Siberia.

132

133 **2. Data and Methods**

134 The Kolyma River in Northeast Siberia is among the six largest arctic rivers and drains a
135 ~650,000 km² region underlain by vast deposits of Holocene-aged peat and Pleistocene-aged
136 loess known as yedoma, much of which is currently stored in ice-rich permafrost throughout the
137 region (Holmes et al., 2012; Holmes et al., 2013). These peats and yedoma deposits are
138 important sources of DOM to terrestrial waters that in turn play a significant role in the transport
139 and ultimate remineralization of organic carbon to atmospheric CO₂ and CH₄ (e.g., Walter et al.,
140 2006; Mann et al., 2012; Denfeld et al., 2013; Spencer et al., 2015). The Kolyma River basin
141 and its subwatersheds exhibit extreme hydrologic seasonality, with ice breakup and peak river
142 discharge typically occurring in late May or early June. In this study, sampling took place along
143 the most northern ~250 km of the Kolyma River in the vicinity of Cherskiy, Sakha Republic,
144 Russia (68.767°N, 161.333°E) during the mid-summer period of July 2009 (Figure 1). Samples

145 were collected over a narrow temporal window from July 11–25, 2009 in order to capture a
146 “snapshot” of observations during the mid-summer period. In total, 47 water samples were
147 collected, including soil pore waters in shallow wetlands (n=9), small streams with watersheds
148 <100 km² (n=15), major river tributaries with watersheds 900–120,000 km² (n=14), and Kolyma
149 mainstem locations with watersheds >400,000 km² (n=9). Although we did not determine
150 residence times directly for our sampled sites, Vonk et al. (2013) estimated that in higher relief
151 areas near Duvannyi Yar (adjacent to the Kolyma River mainstem), the transport time from
152 permafrost thaw to entry into the Kolyma River may be less than one hour. Furthermore, with
153 respect to the mainstem, it has been estimated that water residence times in the Kolyma River
154 from Duvannyi Yar to the river mouth may be ~3–7 days, assuming average mainstem velocities
155 of 0.5–1.5 m/s (Holmes et al., 2012; Vonk et al., 2013). As such, permafrost-derived C may not
156 be easily detectable at the river mouth, as this time is likely comparable to the rapid removal
157 rates of highly labile permafrost C determined through incubation experiments (e.g., Holmes et
158 al., 2012; Vonk et al., 2013).

159 Samples were collected by hand using a 1 L acid-washed high density polyethylene
160 (HDPE) bottle as a collection vessel, where sample waters were used to rinse the bottle several
161 times before filling. Soil pore waters were collected by depressing the soil surface within the
162 wetlands and allowing the water to slowly seep into the collection vessel. In shallow streams,
163 less than 0.5 m in depth, samples were collected approximately midway below the surface and
164 the bottom. In larger tributaries and rivers, samples were collected at a depth of ~0.5 m. Water
165 samples were then filtered through precombusted (450°C for 6 hours) Whatman 0.7 µm GF/F
166 filters in the field and stored in acid-washed HDPE bottles without headspace to minimize
167 degassing and algal growth. Upon returning to the laboratory (typically within ~1 day), DOC

168 samples were acidified with concentrated HCl to a pH of ≤ 2 and stored refrigerated and in the
169 dark until analysis via high-temperature combustion using a Shimadzu TOC-VCPH Analyzer
170 (within one month of collection). DOC was calculated as the mean of 3 to 5 injections with a
171 coefficient of variance less than 2%.

172 We additionally conducted a series of organic matter bioavailability assays to assess the
173 total and relative amounts of bioavailable DOC in soil, stream, and river environments. These
174 assays relied upon 5-day biological oxygen demand (BOD) incubations, with methods similar to
175 those in Mann et al. (2014). Water samples were collected in triplicate glass 300 mL BOD
176 bottles and filtered as DOC (above). The samples were initially allowed to equilibrate via
177 filtering in a controlled laboratory environment at 15°C, after which t=0 was the start time of the
178 incubations. The Winkler titration method was used to measure dissolved oxygen (DO)
179 concentrations initially (t=0) (i.e., in situ DO) as well as after 5-day incubations at 15°C, where
180 bottles were kept in the dark in between measurements. At t=0, DO measurements were at
181 concentrations expected at equilibrium with the 15°C laboratory temperature (~8.5–9.0 mg/L).
182 This temperature was only slightly warmer than environmental sampling conditions (i.e., the
183 Kolyma River mainstem samples ranged from 11.40–13.90°C, river samples ranged from 10.70–
184 14.20°C, and stream samples ranged from 4.40–13.80°C). However, we maintained samples at
185 15°C as is standard in the BOD method, which allowed samples to be treated identically in the
186 controlled experiment (in situ temperatures varied depending not only upon location but also
187 date and time of day). Furthermore, bottles were wrapped tightly with paraffin such that
188 physical degassing should have been minimal during the incubations. BOD was then calculated
189 as the difference between DO concentrations at t = 0 and following the 5-day incubations. We
190 assumed 100% of DO consumed was converted to CO₂ via aerobic respiration and that the

191 carbon source respired was DOM, where resulting BOD measurements were used an analog for
192 bioavailable DOC. The Winkler method we used here has been used extensively and is attractive
193 for a variety of reasons, including: (i) enabling DO to be measured with precision of 0.01 mg/L,
194 thus low respiration rates can be accurately measured; (ii) allowing for convenient replication of
195 assays within habitats; (iii) permitting experimental manipulation of standard bioassays (e.g., N
196 and P amendments, photolysis experiments, alteration of initial microbial consortia, and
197 temperature manipulation; (iv) helping to segregate the relative roles of water column and
198 sediment processes (through comparisons with sediment analyses); and (v) helping to inform
199 more realistic ecosystem-level experiments that are much more laborious and time intensive.

200 In order to investigate the optical characteristics of the DOM in these samples, we
201 additionally measured the ultraviolet-visible absorption spectra of CDOM from this broad
202 collection of waters. CDOM absorbance was measured on filtered (precombusted Whatman 0.7
203 μm GF/F), unacidified waters stored in acid-washed HDPE bottles immediately after collection
204 (within \sim 1 day) at the Northeast Science Station in Cherskiy using a Thermo Scientific
205 GENESYS 10 UV/Vis Spectrophotometer across wavelengths 800–200 nm (1 nm interval) with
206 a 1 cm quartz cuvette. All sample spectra were blank corrected using Milli-Q water (18 Ω).
207 Measurements were made after samples had equilibrated to the laboratory temperature in order
208 to minimize temperature effects. Null-point adjustments were performed on all spectra, such that
209 CDOM absorbance was assumed to be zero across wavelengths greater than 750 nm and the
210 average absorbance between 750 nm and 800 nm was subtracted from each spectrum to correct
211 for offsets owing to instrument baseline drift, temperature, scattering, and refractive effects
212 (Green and Blough, 1994; Helms et al, 2008). CDOM absorption coefficients were calculated
213 as:

214
$$a(\lambda) = 2.303A(\lambda)/l \quad (1)$$

215 where a is the Napierian absorption coefficient (m^{-1}) at a specified wavelength (λ , in nm), $A(\lambda)$ is
216 the absorbance at the wavelength, and l is the cell path length in meters (Green and Blough,
217 1994). To avoid inner-filtering effects, several highly absorbing samples (primarily the soil pore
218 waters) were diluted with Milli-Q water before analysis (to the point where A_{350} was ≤ 0.02 for a
219 1 cm path length) to avoid saturation of the spectra at short wavelengths, where the final CDOM
220 absorbance and therefore absorption coefficients were corrected for these procedures.

221 CDOM spectral slopes (S , nm^{-1}) between 290–350 nm ($S_{290-350}$), 275–295 nm ($S_{275-295}$),
222 and 350–400 nm ($S_{350-400}$), calculated within log-transformed absorption spectra, were also
223 utilized to investigate DOM characteristics of contrasting water types, and were calculated as:

224
$$a(\lambda) = a(\lambda_{ref}) e^{-S(\lambda - \lambda_{ref})} \quad (2)$$

225 where $a(\lambda)$ is the absorption coefficient at a specified wavelength, λ_{ref} is a reference wavelength,
226 and S is the slope fitting parameter (Hernes et al., 2008; Helms et al., 2008; Spencer et al.,
227 2009a). All slopes are reported here as positive values, such that higher (i.e., steeper) slopes
228 indicate a greater decrease in absorption with increasing wavelength. Additional CDOM
229 parameters investigated here include the spectral slope ratio (S_R), calculated as the ratio between
230 $S_{275-295}$ and $S_{350-400}$; the ratio between CDOM absorption coefficients (a) at 250 nm and 365 nm
231 ($a_{250}:a_{365}$); and specific UV absorbance (SUVA_{254}), determined by dividing UV absorbance (A)
232 at 254 nm by the sample DOC concentration and reported in units of $\text{L mg C}^{-1} \text{ m}^{-1}$ (Weishaar et
233 al., 2003). These six CDOM parameters ($S_{290-350}$, $S_{275-295}$, $S_{350-400}$, $a_{250}:a_{365}$, SUVA_{254} , and S_R)
234 have been shown to provide insights for various DOM characteristics such as molecular weight,
235 source waters, composition, age, and aromatic content for a variety of geographic regions (e.g.,
236 Weishaar 2003; Neff et al., 2006; Helms et al., 2008; Spencer et al., 2008; Spencer et al., 2009a;

237 Spencer et al., 2009b; Mann et al., 2012). As such, we chose our method for spectral slope
238 calculations to be consistent with previous studies to foster intercomparisons between datasets,
239 however future studies may derive further insight utilizing methods that calculate a continuous
240 spectral slope curve over the full 200–800 nm span (e.g., Loiselle et al., 2009) rather than only
241 specific wavelength intervals as presented here.

242

243 **3. Results**

244 Total DOC concentrations (and the variance among values within each water type)
245 decreased markedly downstream along the flow-path continuum from soil pore waters to the
246 Kolyma River mainstem (Figure 2a). Mean (± 1 standard deviation) DOC values were $43.3 \pm$
247 22.8 mg L^{-1} (soil pore waters), $11.6 \pm 3.0 \text{ mg L}^{-1}$ (streams), $4.9 \pm 1.6 \text{ mg L}^{-1}$ (rivers), and $3.6 \pm$
248 0.4 mg L^{-1} (mainstem waters). Soil pore waters, in particular, showed highly variable DOC
249 concentrations (ranging from 13.2 to 64.7 mg L^{-1}) demonstrating the heterogeneous supply of
250 DOM from terrestrial systems to streams. By contrast, DOC concentrations in the Kolyma
251 mainstem along the ~250 km stretch sampled were remarkably similar (ranging from 3.0 to 4.4
252 mg L^{-1}) during this mid-summer July period (Figure 2a). Furthermore, DOC concentrations of
253 the four water types sampled were found to be significantly different from one another (one-way
254 ANOVA, $p < 0.05$).

255 Concentrations of bioavailable DOC showed similar patterns to DOC, declining
256 downstream along the flow-path continuum with increasing water residence time in the system
257 (Figure 2b). Bioavailable DOC concentrations averaged $0.9 \pm 0.2 \text{ mg L}^{-1}$ (soil pore waters), 0.3
258 $\pm 0.1 \text{ mg L}^{-1}$ (streams), $0.3 \pm 0.2 \text{ mg L}^{-1}$ (rivers), and $0.2 \pm 0.2 \text{ mg L}^{-1}$ (mainstem waters), and
259 showed relative greater variability than DOC within the stream, river and mainstem water types.

260 Concentrations of bioavailable DOC in soil pore waters were statistically different from the other
261 three water types (one-way ANOVA, $p < 0.05$), although by contrast, streams, rivers, and
262 mainstem waters were not statistically different from one another ($p > 0.05$). Importantly, the
263 percentage of bioavailable DOC (i.e., calculated as the amount of bioavailable DOC divided by
264 total DOC) did not significantly decrease downstream (one-way ANOVA, $p > 0.05$) and showed
265 relatively similar values among the four water sample types along the flow-path continuum
266 (Figure 2c), where percentages averaged $3.9 \pm 3.8\%$ (soil pore waters), $3.2 \pm 1.9\%$ (streams), 6.2
267 $\pm 4.3\%$ (rivers), and $4.5 \pm 4.5\%$ (mainstem waters).

268 CDOM absorption spectra (200–800 nm) showed clear separation between soil pore
269 waters, streams, rivers, and the Kolyma mainstem, where soil pore waters exhibited values
270 markedly higher than the other three water sample types (Figure 3a). CDOM absorption also
271 clearly declined downstream from streams, rivers, to mainstem waters when assessing those
272 waters only (Figure 3b). Furthermore, we investigated the potential for utilizing CDOM
273 absorption as a proxy for DOC concentrations in these waters. Our data revealed that
274 independent of water type along the stream-river-mainstem flow-path, CDOM absorption was
275 strongly linearly correlated to DOC concentrations at 254, 350, and 440 nm (Figure 4). In
276 particular, CDOM absorption at 254 nm had the highest predictive capability of DOC ($r^2 =$
277 0.958 , $p < 0.01$), with CDOM absorption at 350 nm ($r^2 = 0.855$, $p < 0.01$) and 440 nm ($r^2 = 0.667$,
278 $p < 0.01$) less strongly predictive (Figure 4).

279 We additionally investigated the quantitative distribution of the six derived CDOM
280 parameters ($S_{290-350}$, $S_{275-295}$, $S_{350-400}$, $a_{250}:a_{365}$, $SUVA_{254}$, and S_R) across the four water types
281 (Figure 5; Table 1). In general, four parameters ($S_{290-350}$, $S_{275-295}$, $a_{250}:a_{365}$, and S_R) showed an
282 increasing pattern along the flow-path continuum, whereas two parameters ($S_{350-400}$ and

283 SUVA₂₅₄) showed a decreasing pattern. In terms of whether the values of the six parameters
284 were statistically significantly different among water sample types, one-way ANOVA tests (at
285 the 0.05 level) revealed inconsistent results. Most commonly, soil pore waters were statistically
286 different from all other water types for four of the parameters ($S_{290-350}$, $S_{275-295}$, $a_{250}:a_{365}$, and S_R),
287 but no consistent pattern was observed in significant differences across other water types.
288 However, the spectral slope ratio (S_R) was the only CDOM parameter of the six investigated that
289 showed statistically significant differences between all four water types ($p < 0.05$).

290 Lastly, we examined the relationships between CDOM optical properties and DOM
291 bioavailability. To this end, we performed linear regressions between all six of our derived
292 CDOM parameters and bioavailable DOC concentrations to determine the strength of their
293 ability to predict bioavailable DOC. Our results indicated that five of the CDOM parameters
294 ($S_{290-350}$, $S_{275-295}$, $a_{250}:a_{365}$, SUVA₂₅₄, and S_R) were statistically significant predictors at the 0.05
295 level (Table 2). In particular, S_R showed the strongest relationship with bioavailable DOC
296 concentrations (r^2 value = 0.45, $p < 0.01$). The relationship between bioavailable DOC
297 concentrations and S_R (Figure 6) showed a distinct negative trend (bioavailable DOC mg L⁻¹ = -
298 2.204(S_R) + 2.518), with the highest bioavailable DOC concentrations and lowest S_R values for
299 soil pore waters, and lowest bioavailable DOC concentrations and highest S_R values for Kolyma
300 River mainstem waters. We found a clear gradation in the relationship between S_R and
301 bioavailable DOC down the flow-path continuum, as one would also expect by examining these
302 parameters individually (e.g., Figures 2b, 5f). In summary, not only was S_R the only CDOM
303 parameter that showed statistically significant separation between all four water types examined,
304 but it also had the strongest relationship when compared with concentrations of bioavailable
305 DOC.

306 **4. Discussion and Conclusions**

307 In this study, we present a full suite of DOC, bioavailable DOC, and CDOM parameters
308 throughout the permafrost-dominated Kolyma River basin in Northeast Siberia with the purpose
309 of helping to elucidate the processing of DOM along a full flow-path continuum from soil pore
310 waters to the mainstem. Our findings show that average concentrations of DOC and bioavailable
311 DOC generally decrease as waters travel downstream from soil pore waters, streams, rivers, and
312 ultimately to the Kolyma River mainstem. This pattern suggests the occurrence of rapid in-
313 stream processing of DOM and potential remineralization of DOC to atmospheric CO₂ during
314 this July baseflow period well before these waters reach the Arctic Ocean (e.g., Denfeld et al.,
315 2013; Mann et al., 2015; Spencer et al., 2015). The amount of total DOC putatively lost to
316 remineralization is a relatively small fraction (~3–6% depending upon water type), but on par
317 with similar studies across the Arctic for this time of year (e.g., Holmes et al., 2008). Although
318 this may be a relatively small proportion, it is likely the permafrost-derived, ancient DOC found
319 in headwaters that is contributing to permafrost carbon feedbacks to climate warming (Mann et
320 al., 2015). Moving downstream, the river continuum concept predicts that relative diversity of
321 organic molecules decreases from the headwaters to the river mouth (Vannote et al., 1980). As
322 energetically favorable compounds are converted to living tissue or respired as CO₂, bulk DOM
323 in the Kolyma basin has indeed been shown in previous studies to become less diverse moving
324 from headwaters to mainstem waters before exported to the Arctic Ocean (Spencer et al., 2015).

325 CDOM parameters presented in this study give further insight into characteristics of
326 DOM along the full flow-path continuum throughout the Kolyma River basin. For instance, the
327 specific ultraviolet absorbance (SUVA₂₅₄) has been shown to be correlated with DOM
328 composition, where SUVA₂₅₄ values are positively correlated with percent aromaticity and

329 molecular size of DOM (and for a given river have been shown to be greatest during spring
330 flood) (e.g., Weishaar et al., 2003; Spencer et al., 2009a; Mann et al., 2012). In this study, we
331 generally found progressively decreasing SUVA₂₅₄ values along the flow-path from soil pore
332 waters towards mainstem waters, suggesting that soil pore waters contain higher molecular
333 weight, aromatic terrestrial DOM that generally becomes lower in molecular weight and
334 aromaticity along the flow-path continuum towards the Kolyma River mainstem. In addition, the
335 $a_{250}:a_{365}$ ratio has been shown to be negatively correlated to aromaticity and molecular size of
336 DOM (Peuravuori and Pihlaja, 1997). In fact (similar to samples from the Yukon River, Alaska
337 (Spencer et al., 2009a)), our data showed that the $a_{250}:a_{365}$ ratio is significantly negatively
338 correlated with SUVA₂₅₄ ($a_{250}:a_{365} = -0.947 (\text{SUVA}_{254}) - 0.947; r^2=0.49, p<0.01$). As such, the
339 $a_{250}:a_{365}$ ratio may potentially be utilized as a first-order proxy for SUVA₂₅₄ when DOC
340 concentrations cannot be easily determined.

341 However, despite our observations of downstream shifts in DOM composition, we find a
342 relatively constant proportion of DOC that was bioavailable (~3–6% of total DOC) regardless of
343 relative water residence time along the flow-path. This suggests that continual microbial
344 processing of organic matter is able to occur with similar rates during transit from headwaters
345 throughout the Kolyma River drainage network to the Arctic Ocean concurrent with ongoing
346 downstream CDOM compositional changes. Microbial demand in headwater streams of the
347 Kolyma River basin is subsidized by significant quantities of DOC specifically derived from
348 permafrost and aged soils, yet the proportion of permafrost supporting DOC mineralization
349 declines as waters move downstream through the fluvial network (Mann et al., 2015). Thus, our
350 results importantly show that microbial metabolism continues at similar rates independent of
351 dominant DOM source and radiocarbon age.

352 There may be several reasons for why microbial metabolism maintains this consistent
353 rate along the flow-path, including the possibility that aquatic microorganisms are acclimating to
354 a downstream shift in DOM composition. The higher overall amounts of bioavailable DOC we
355 measured in soil pore waters may reflect a highly bioreactive permafrost or aged surface soil
356 derived fraction of the bulk DOC pool (e.g., Vonk et al., 2013; Mann et al., 2014). Further
357 downstream in larger tributary and Kolyma mainstem waters, it has been shown that lower total
358 amounts of bioavailable DOC is supported almost entirely from predominantly modern
359 radiocarbon aged surface soils and vegetation sources (Mann et al., 2015). Aquatic
360 microorganisms may therefore be readily acclimating to significant shifts in DOM composition
361 caused by selective losses of unique DOM fractions (e.g., Kaplan and Bott, 1983; Spencer et al.,
362 2015) alongside high-internal demand for labile DOM by stream communities in lower order
363 streams, which would otherwise generally be expected to result in decreased DOM lability with
364 increasing water residence time (Stepanauskas et al., 1999a,b; Wikner et al., 1999; Langenheder
365 et al., 2003; Sondergaard et al., 2003; Fellman, 2010; Fellman et al., 2014).

366 Additional mechanisms such as increasing photodegradation downstream may also
367 account for our observed patterns in downstream DOM. Previous studies have indicated that
368 CDOM spectral slopes (particularly $S_{290-350}$ and $S_{275-295}$) can serve as indicators of DOM source
369 and composition, where a steeper spectral slope typically suggests lower molecular weight
370 material with decreasing aromatic content and a shallower (i.e., lower) slope typically suggests
371 higher molecular weight material with increasing aromatic content (Green and Blough, 1994;
372 Blough and Del Vecchio, 2002; Helms et al., 2008; Spencer et al., 2008; Spencer et al., 2009a).
373 Furthermore, $S_{275-295}$ has been identified as a reliable proxy for dissolved lignin and therefore
374 terrigenous DOM supply across Arctic Ocean coastal waters, as well as photobleaching history

375 (Helms et al., 2008; Fichot et al., 2013). We found a general increase in $S_{290-350}$ and $S_{275-295}$
376 moving downstream through the network, indicative of progressive photodegradation of DOM
377 alongside likely reductions in average DOM molecular weight and aromaticity. We found
378 spectral slopes over longer wavelength regions ($S_{350-400}$) decreased through the network, also
379 suggesting constant photochemical degradation of DOM as waters flowed downstream (e.g.,
380 Helms et al., 2008). The slope ratio (S_R) has also been shown to be a proxy for DOM molecular
381 weight and source, where low ratios typically correspond to more allochthonous, higher
382 molecular weight DOM (Helms et al., 2008; Spencer et al., 2009b; Mann et al., 2012). The
383 advantage of S_R ratios over individual S values is apparent when each spectral slope responds to
384 a process in an opposing manner, emphasizing the response in calculated S_R values. The clear
385 increases in S_R we observed moving downstream in the fluvial network (from a minimum of 0.74
386 in soil pore waters to a maximum of 1.24 in the mainstem) indicate that during July summer
387 conditions, soil pore waters contain higher molecular weight, aromatic terrestrial DOM that
388 generally becomes lower in average molecular weight and aromaticity along the flow-path
389 continuum towards the Kolyma River mainstem. The maximum S_R value of 1.24 we report in
390 the Kolyma River mainstem is markedly higher than the range of S_R (0.82–0.92) reported in
391 Stedmon et al. (2011) for the Kolyma from 2004 and 2005, demonstrating the heterogeneity of
392 DOM properties even in mainstem waters and the necessity for greater temporal resolution in
393 monitoring. Similar to spectral slopes, S_R values may also be indicative of photobleaching
394 history (e.g., Helms et al., 2008) and our we observed increase in S_R downstream through the
395 network suggests evidence of on-going photochemical degradation of surface water DOM during
396 transit.

397 Photodegradation may indeed play an important and direct role in our observed consistent
398 fraction of bioavailable DOC along the flow-path. Previous studies in the Arctic underscore the
399 importance of residence times as well as a significant combined role for photo- and biological
400 degradation along the flow-path in Arctic watersheds (Cory et al., 2007; Merck et al., 2012; Cory
401 et al., 2013; Laurion and Mladenov, 2013). These previous results show that the photochemical
402 “pretreatment” of stream DOM that occurs during export into lakes and coastal zones may
403 impact the ability of microorganisms to mineralize DOM. Therefore, the residence times and
404 flow-paths of waters should greatly influence the ultimate fate of DOM (e.g., DOM vs. CO₂)
405 exported to the adjacent ocean. In our case, we find that our increasing S_R values downstream
406 suggest important photodegradation processes are occurring along the flow-path continuum,
407 where this photodegradation may potentially release significant quantities of labile DOM for
408 continued microbial processing of DOM further downstream in these stream networks. In other
409 words, our results suggest that more abundant newly exposed bioavailable molecules upstream
410 are replaced downstream by photobleached smaller molecules (originating from aromatic
411 compounds), resulting in the fraction of DOC used relatively constant without any clear pattern
412 overall. If this were not the case, we would expect to see a declining fraction of bioavailable
413 DOC along the flow-path continuum.

414 In this study, we have provided new and important findings with regards to the spatial
415 distribution of DOM concentration, bioavailability, and optical properties during mid-summer
416 hydrologic conditions throughout the Kolyma River basin in Northeast Siberia. Freshwater DOC
417 measurements across the network were strongly positively correlated to CDOM absorption at
418 254 nm ($r^2 = 0.958$, $p < 0.01$), confirming the utility of simple CDOM optical measurements for
419 estimating carbon concentrations in arctic freshwaters (Spencer et al., 2008, 2009a; Stedmon et

420 al., 2011) and across water types within the Kolyma River basin in particular. Furthermore, the
421 optical parameter S_R proved to be the only CDOM compositional measure that showed
422 statistically significant separation between all four water types examined during the study period,
423 suggesting that this parameter may be useful for easily distinguishing characteristics and
424 processes occurring in organic matter among water types along the full flow-path continuum.
425 The significant increase in S_R values we observed downstream through the network suggests
426 evidence of on-going photochemical degradation of surface water DOM during transit.
427 Additionally, of all the CDOM parameters, S_R values were most closely related to concentrations
428 of bioavailable DOC ($r^2 = 0.454$, $p < 0.01$), suggesting that this value may be correlated with a
429 decline in bioavailable DOC through the network. However, biological degradation has
430 previously been shown to typically slightly decrease S_R values (Helms et al., 2008), which
431 indicates that the opposite relationship observed here may instead be a consequence of co-
432 variance with photodegradation of DOM, or demonstrate that S_R values may reflect a broader,
433 more complex range of physical and biological processes than previously recognized. Garnering
434 further insight from our measurements, the relatively constant proportion of DOC that was
435 bioavailable regardless of relative water residence time along the flow-path may be a
436 consequence of two potential scenarios allowing for continual processing of organic material
437 within the system, namely: (a) aquatic microorganisms are acclimating to a downstream shift in
438 DOM composition; and/or (b) photodegradation is continually generating labile DOM for
439 continued microbial processing of DOM along the flow-path continuum. Without such
440 processes, we would otherwise expect to see a declining fraction of bioavailable DOC
441 downstream with increasing residence time of water in the system.

442 Unlike many previous studies that focus on only mainstem rivers in the Arctic, we focus
443 here on a variety of waters along a full flow-path continuum, showing that CDOM metrics (in
444 particular, S_R) reflect important compositional differences in DOM of waters along the transit
445 from headwaters to the Arctic Ocean. The range in DOM properties of waters travelling
446 downstream through the Kolyma Basin often spanned wider ranges than DOM compositional
447 differences reported annually among the six major arctic rivers. For example, S_R values across
448 the major arctic rivers over the years 2004 and 2005 spanned a minimum of 0.79 in the Yenisey
449 River, to a maximum value of 1.11 in the Mackenzie River (Stedmon et al., 2011), compared to
450 the range of 0.74–1.24 for waters in our study within a single basin. It is therefore essential that
451 changes taking place in the quality of CDOM exported by these rivers be examined throughout
452 entire river basins in order to adequately assess climate driven shifts in terrigenous carbon supply
453 and reactivity. Future work that includes both photo- and microbial degradation experiments
454 may further elucidate the ability for S_R to serve as a direct proxy for these processes along a
455 flow-path gradient. Our overall results thus far demonstrate promise for utilizing ultraviolet-
456 visible absorption characteristics to easily, inexpensively, and comprehensively monitor the
457 quantity and quality of DOM (over broad ranges) across permafrost landscapes in the Arctic.
458 This is particularly critical for remote arctic landscapes such as those in Northeast Siberia, where
459 the future fate of organic carbon currently frozen in permafrost soils (and whether it ultimately is
460 released as CO_2 and CH_4) is tightly linked to the lability of this material.

461

462 **Acknowledgements**

463 This research was part of the Polaris Project (www.thepolarisproject.org), supported
464 through grants from the National Science Foundation Arctic Sciences Division (Grants ARC-

465 1044560 and DUE-0732586 to K. Frey and Grants ARC-1044610 and DUE-0732944 to R.
466 Holmes). We thank E. Bulygina, A. Bunn, B. Denfeld, S. Davydov, A. Davydova, M. Hough, J.
467 Schade, E. Seybold, N. Zimov, and S. Zimov for assistance with field sampling collections
468 and/or overall project coordination. We additionally thank Isabelle Laurion and two anonymous
469 reviewers for their constructive comments and suggestions on an earlier version of this
470 manuscript.

471

472

473

474

475

476

477

478

479

480

481

482

483

484

485

486

487

488 **References Cited**

489

490 Battin, T. J., Kaplan, L. A., Findlay, S., Hopkinson, C. S., Marti, E., Packman, A. I., Newbold, J.
491 D., and Sabater, F.: Biophysical controls on organic carbon fluxes in fluvial networks, *Nature*
492 *Geoscience*, 1, 95–100, 2009a.

493

494 Battin, T. J., Luysaert, S., Kaplan, L. A., Aufdenkampe, A. K., Richter, A., and Tranvik, L. J.:
495 The boundless carbon cycle, *Nature Geoscience*, 2, 598–600, 2009b.

496

497 Blough, N. V. and Del Vecchio, R.: Chromophoric DOM in the coastal environment, in
498 *Biogeochemistry of Marine Dissolved Organic Matter*, edited by D. A. Hansell and C. A.
499 Carlson, pp. 509–546, Elsevier, San Diego, California, 2002.

500

501 Bronk D. A.: Dynamics of DON, in: *Biogeochemistry of Marine Dissolved Organic*
502 *Matter*, edited by: Hansell, D. A. and Carlson, C. A., Academic Press, San Diego, pp. 153–249,
503 2002.

504

505 Chin, Y. P., Traina, S. J., Swank, C. R., and Backhus, D.: Abundance and properties of dissolved
506 organic matter in pore waters of a freshwater wetland, *Limnology and Oceanography*, 43(6),
507 1287–1296, 1998.

508

509 Cole, J. J., Prairie, Y. T., Caraco, N. F., McDowell, W. H., Tranvik, L. J., Striegl, R. G., Duarte,
510 C. M., Kortelainen, P., Downing, J. A., Middelburg, J. J., and Melack, J.: Plumbing the global
511 carbon cycle: Integrating Inland Waters into the Terrestrial Carbon Budget. *Ecosystems*, 10,
512 171–184, 2007.

513

514 Cory, R. M., Crump, B. C., Dobkowski, J. A., and Kling, G. W.: Surface exposure to sunlight
515 stimulates CO₂ release from permafrost soil carbon in the Arctic, *Proceedings of the National*
516 *Academy of Sciences*, 110(9), 3429–3434, 2013.

517

518 Cory, R. M., McKnight, D. M., Chin, Y.-P., Miller, P., and Jaros, C. L.: Chemical characteristics
519 of fulvic acids from Arctic surface waters: Microbial contributions and photochemical
520 transformations, *J. Geophys. Res.*, 112, G04S51, doi:10.1029/2006JG000343, 2007.

521

522 Cory, R. M., Ward, C. P., Crump, B. C. and Kling, G. W.: Sunlight controls water column
523 processing of carbon in arctic fresh waters, *Science*, 345(6199), 925–928,
524 doi:10.1126/science.1253119, 2014.

525 Denfeld, B. A., Frey, K. E., Sobczak, W. V., Mann, P. J., and Holmes, R. M.: Summer CO₂
526 evasion from streams and rivers in the Kolyma River basin, north-east Siberia, *Polar Research*,
527 32, 19704, <http://dx.doi.org/10.3402/polar.v32i0.19704>, 2013.

528

529 Fellman, J. B., Spencer, R. G. M., Hernes, P. J., Edwards, R. T., D'Amore, D. V., and Hood, E.:
530 The impact of glacier runoff on the biodegradability and biochemical composition of terrigenous
531 dissolved organic matter in near-shore marine ecosystems, *Marine Chemistry*, 121, 112–122,
532 2010.

533
534 Fellman, J. B., Spencer, R. G. M., Raymond, P. A., Pettit, N. E., Skrzypek, G., Hernes, P. J., and
535 Grierson, P. F.: Dissolved organic carbon biolability decreases along with its modernization in
536 fluvial networks in an ancient landscape, *Ecology*, 95(9), 2622–2632, 2014.

537
538 Fichot, C. G., Kaiser, K., Hooker, S. B., Zmon, R. M. W., Babin, M., Belanger, S., Walker, S.
539 A., and Benner, R.: Pan-Arctic distributions of continental runoff in the Arctic Ocean, *Scientific*
540 *Reports*, 3, doi:10.1038/srep01053, 2013.

541
542 Frey, K. E. and McClelland, J. W.: Impacts of permafrost degradation on arctic river
543 biogeochemistry, *Hydrological Processes*, 23, 169–182, 2009.

544
545 Frey, K. E., Siegel, D. I., and Smith, L. C.: Geochemistry of West Siberian streams and their
546 potential response to permafrost degradation, *Water Resources Research*, 43, W03406,
547 doi:10.1029/2006WR004902, 2007.

548
549 Frey, K. E. and Smith, L. C.: Amplified carbon release from vast West Siberian peatlands by
550 2100, *Geophysical Research Letters*, 32, L09401, doi:10.1029/2004GL022025, 2005.

551
552 Green, S. A., and Blough, N. V.: Optical absorption and fluorescence properties of chromophoric
553 dissolved organic matter in natural waters, *Limnology and Oceanography*, 39, 1903–1916, 1994.

554
555 Hayes, D. J., Kicklighter, D. W., McGuire, A. D., Chen, M., Zhuang, Q. L., Yuan, F. M.,
556 Melillo, J. M., and Wullschlegel, S. D.: The impacts of recent permafrost thaw on land-
557 atmosphere greenhouse gas exchange, *Environmental Research Letters*, 9(4), doi: 10.1088/1748-
558 9326/9/4/045005, 2014.

559
560 Helms, J. R., Stubbins, A., Ritchie, J. D., Minor, E. C., Kieber, D. J., and Mopper, K.:
561 Absorption spectral slopes and slope ratios as indicators of molecular weight, source, and
562 photobleaching of chromophoric dissolved organic matter, *Limnol. Oceanogr.*, 53, 955–969,
563 2008.

564
565 Hernes, P. J., Spencer, R. G. M., Dyda, R. Y., Pellerin, B. A., Bachand, P. A. M., and
566 Bergamaschi, B. A.: The role of hydrologic regimes on dissolved organic carbon composition in
567 an agricultural watershed, *Geochimica et Cosmochimica Acta*, 72, 5266–5277, 2008.

568
569 Holmes, R. M., McClelland, J. W., Peterson, B. J., Tank, S. E., Bulygina, E., Eglinton, T. I.,
570 Gordeev, V. V., Gurtovaya, T. Y., Raymond, P. A., Repeta, D. J., Staples, R., Striegl, R. G.,
571 Zhulidov, A. V., and Zimov, S. A.: Seasonal and annual fluxes of nutrients and organic matter
572 from large rivers to the Arctic Ocean and surrounding seas, *Estuaries and Coasts*, 35, 369–382,
573 doi:10.1007/s12237-011-9386-6, 2012.

574
575 Holmes, R. M., Coe, M. T., Fiske, G. J., Gurtovaya, T., McClelland, J. W., Shiklomanov, A. I.,
576 Spencer, R. G. M., Tank, S. E., and Zhulidov, A. V.: Climate change impacts on the hydrology
577 and biogeochemistry of Arctic Rivers, in *Global Impacts of Climate Change on Inland Waters*,
578 edited by C. R. Goldman, M. Kumagai, and R. D. Robarts, Wiley, 2013.

579
580 Holmes, R. M., McClelland, J. W., Raymond, P. A., Frazer, B. B., Peterson, B. J., and Stieglitz,
581 M.: Lability of DOC transported by Alaskan rivers to the Arctic Ocean, *Geophysical Research*
582 *Letters*, 35, L03402, doi:10.10289/2007GL032837, 2008.

583
584 Judd, K. E. and Kling, G. W.: Production and export of dissolved C in arctic tundra mesocosms:
585 the roles of vegetation and water flow, *Biogeochemistry*, 60, 213–234, 2002.

586
587 Kaplan, L. A. and Bott, T. L.: Microbial heterotrophic utilization of dissolved organic matter in a
588 piedmont stream, *Freshwater Biology*, 13, 363–377, 1983.

589
590 Karl, D. M. and Björkman, K. M.: Dynamics of DOP. In: Hansell, D., Carlson, C. (Eds.),
591 *Biogeochemistry of Marine Dissolved Organic Matter*, Academic Press, San Diego, pp. 249–
592 366, 2002.

593
594 Langenheder, S., Kisand, V., Wikner, J., and Tranvik, L. J.: Salinity as a structuring factor for
595 the composition and performance of bacterioplankton degrading riverine DOC, *FEMS*
596 *Microbiology Ecology*, 45(2), 189–202, 2003.

597
598 Laurion, I. and N. Mladenov: Dissolved organic matter photolysis in Canadian arctic thaw
599 ponds, *Environmental Research Letters*, 8, 035026, 2013.

600
601 Loiselle, S. A., Bracchini, L., Dattilo, A. M., Ricci, M., Tognazzi, A., Cozar, A., and Rossi, C.:
602 Optical characterization of chromophoric dissolved organic matter using wavelength distribution
603 of absorption spectral slopes, *Limnology and Oceanography*, 54(2), 590–597, 2009.

604
605 Mann, P. J., Davydova, A., Zimov, N., Spencer, R. G. M., Davydov, S., Bulygina, E., Zimov, S.,
606 and Holmes, R. M.: Controls on the composition and lability of dissolved organic matter in
607 Siberia’s Kolyma River basin, *Journal of Geophysical Research-Biogeosciences*, 117, G01028,
608 doi:10.1029/2011JG001798, 2012.

609
610 Mann, P. J., Sobczak, W. V., LaRue, M. M., Bulygina, E., Davydova, A., Vonk, J., Schade, J.,
611 Davydov, S., Zimov, N., Holmes, R. M., and Spencer, R. G. M.: Evidence for key enzymatic
612 controls on metabolism of Arctic river organic matter, *Global Change Biology*, 20(4), 1089–
613 1100, 2014.

614
615 Mann, P. J., Eglinton, T. I., McIntyre, C. P., Zimov, N., Davydova, A., Vonk, J. E., Holmes, R.
616 M., and Spencer, R. G. M.: Utilization of ancient permafrost carbon in headwaters of Arctic
617 fluvial networks, *Nature Communications*, doi:10.1038/ncomms8856, 2015.

618
619 McClelland, J. W., Holmes, R. M., Dunton, K. H., and Macdonald, R. W.: The Arctic Ocean
620 Estuary, *Estuaries and Coasts*, 35(2), 353–368, 2012.

621
622 Merck M., Neilson, B., Cory, R., and Kling, G.: Variability of in-stream and riparian storage in a
623 beaded arctic stream. *Hydrological Processes*, 26, 2938–2950, 2012.

624

625 Moran, M. A. and Zepp, R. G.: Role of photoreactions in the formation of biologically labile
626 compounds from dissolved organic matter, *Limnology and Oceanography*, 42(6), 1307–1316,
627 1997.
628

629 Mulholland, P. J.: Dissolved organic matter concentrations and flux in streams, *Journal of the*
630 *North American Benthological Society*, 16(1), 131–141, 1997.
631

632 Neff, J. C., Finlay, J. C., Zimov, S. A., Davydov, S. P., Carrasco, J. J., Schuur, E. A. G., and
633 Davydova, A. I.: Seasonal changes in the age and structure of dissolved organic carbon in
634 Siberian rivers and streams, *Geophysical Research Letters*, 33, L23401,
635 doi:10.1029/2006GL028222, 2006.
636

637 Peuravuori, J. and Pihlaja, K.: Molecular size distribution and spectroscopic properties of aquatic
638 humic substances, *Anal. Chim. Acta*, 337, 133–149, 1997.
639

640 Schreiner, K. M., Bianchi, T. S., and Rosenheim, B. E.: Evidence for permafrost thaw and
641 transport from an Alaskan North Slope watershed, *Geophysical Research Letters*, 41(9), 3117–
642 3126, 2014.
643

644 Sholkovitz, E. R.: Flocculation of dissolved organic and inorganic matter during mixing of river
645 water and seawater, *Geochimica et Cosmochimica Acta*, 40(7), 831–845, 1976.
646

647 Sondergaard, M., Stedmon, C. A., and Borch, N. H.: Fate of terrigenous dissolved organic matter
648 (DOM) in estuaries: Aggregation and bioavailability, *Ophelia*, 57(3), 161–176, 2003.
649

650 Spencer, R. G. M., Aiken, G. R., Butler, K. D., Dornblaser, M. M., Striegl, R. G., and Hernes, P.
651 J.: Utilizing chromophoric dissolved organic matter measurements to derive export and reactivity
652 of dissolved organic carbon exported to the Arctic Ocean: A case study of the Yukon River,
653 Alaska, *Geophysical Research Letters*, 36, L06401, doi:10.1029/2008GL036831, 2009a.
654

655 Spencer, R. G. M., Aiken, G. R., Wickland, K. P., Striegl, R. G., and Hernes, P. J.: Seasonal and
656 spatial variability in dissolved organic matter quantity and composition from the Yukon River
657 basin, Alaska, *Global Biogeochemical Cycles*, 22, GB4002, doi:10.1029/2008GB003231, 2008.
658

659 Spencer, R. G. M., Mann, P. J., Dittmar, T., Eglinton, T. I., McIntyre, C., Holmes, R. M., Zimov,
660 N., and Stubbins, A.: Detecting the signature of permafrost thaw in Arctic rivers, *Geophysical*
661 *Research Letters*, 42, 1–6, doi:10.1002/(ISSN)1944-8007, 2015.
662

663 Spencer, R. G. M., Stubbins, A., Hernes, P. J., Baker, A., Mopper, K., Aufdenkampe, A. K.,
664 Dyda, R. Y., Mwamba, V. L., Mangangu, A. M., Wabakanghanzi, J. N., and Six, J.:
665 Photochemical degradation of dissolved organic matter and dissolved lignin phenols from the
666 Congo River, *Journal of Geophysical Research*, 114, G03010, doi:10.1029/2009JG000968,
667 2009b.
668

669 Stedmon, C. A., Amon, R. M. W., Rinehart, A. J., and Walker, S. A.: The supply and
670 characteristics of colored dissolved organic matter (CDOM) in the Arctic Ocean: Pan Arctic
671 trends and differences, *Marine Chemistry*, 124, 108–118, 2011.

672
673 Stepanauskas, R., Edling, H., and Tranvik, L. J.: Differential dissolved organic nitrogen
674 availability and bacterial smniopeptidase activity in limnic and marine waters, *Microbial
675 Ecology*, 38(3), 264–272, 1999a.

676
677 Stepanauskas, R., Leonardson, L., and Tranvik, L. J.: Bioavailability of wetland-derived DON to
678 freshwater and marine bacterioplankton, *Limnology and Oceanography*, 44(6), 1477–1485,
679 1999b.

680
681 Tesi, T., Semiletov, I., Hugelius, G., Dudarev, O., Kuhry, P., and Gustafsson, O.: Composition
682 and fate of terrigenous organic matter along the Arctic land-ocean continuum in East Siberia:
683 Insights from biomarkers and carbon isotopes, *Geochimica et Cosmochimica Acta*, 133, 235–
684 256, 2014.

685
686 Vannote, R. L., Minshall, G. W., Cummins, K. W., Sedell, J. R., and Cushing, C. E.: The River
687 Continuum Concept, *Canadian Journal of Fisheries and Aquatic Sciences*, 37, 130–137, 1980.

688
689 Vonk, J. E., Mann, P. J., Davydov, S., Davydova, A., Spencer, R. G. M., Schade, J., Sobczak, W.
690 V., Zimov, N., Bulygina, E., Eglinton, T. I., and Holmes, R. M.: High biolability of ancient
691 permafrost carbon upon thaw, *Geophysical Research Letters*, 40, 2689–2693, 2013.

692
693 Wachenfeldt, E. von, Bastviken, D., and Tranvika, L. J.: Microbially induced flocculation of
694 allochthonous dissolved organic carbon in lakes. *Limnology and Oceanography*, 54, 1811–1818,
695 2009.

696
697 Walter, K. M., Zimov, S. A., Chanton, J. P., Verbyla, D., and Chapin III, F. S.: Methane
698 bubbling from Siberian thaw lakes as a positive feedback to climate warming, *Nature*, 443, 71–
699 75, 2006.

700
701 Webster, J. R. and Meyer, J. L.: Organic matter budgets for streams: A synthesis, *Journal of the
702 North American Benthological Society*, 16(1), 141–161, 1997.

703
704 Weishaar, J. L., Aiken, G. R., Bergamaschi, B. A., Fram, M. S., Fujii, R., and Mopper, K.:
705 Evaluation of specific ultraviolet absorbance as an indicator of the chemical composition and
706 reactivity of dissolved organic carbon, *Environ. Sci. Technol.*, 37, 4702–4708, 2003.

707
708 Wikner, J., Cuadros, R., and Jansson, M.: Differences in consumption of allochthonous DOC
709 under limnic and estuarine conditions in a watershed, *Aquatic Microbial Ecology*, 17(3), 289–
710 299, 1999.

711
712
713
714

715 **Table 1.** Mean spectral slope and other CDOM parameters for soil pore waters, streams, rivers,
 716 and the Kolyma River mainstem.

717

	$S_{290-350}$ ($\times 10^{-3} \text{ nm}^{-1}$)	$S_{275-295}$ ($\times 10^{-3} \text{ nm}^{-1}$)	$S_{350-400}$ ($\times 10^{-3} \text{ nm}^{-1}$)	$a_{250}:a_{365}$	SUVA_{254} ($\text{L mg C}^{-1} \text{ m}^{-1}$)	S_R
Soil pore waters	15.35	15.27	18.65	5.47	3.52	0.82
Streams	17.08	17.39	18.89	6.44	2.94	0.92
Rivers	17.17	17.79	18.19	6.27	2.77	0.98
Kolyma Mainstem	18.10	18.57	17.50	6.53	2.56	1.06

718

719

720

721

722 **Table 2.** Relationships between bioavailable DOC and each of the six CDOM metrics

723 investigated. S_R shows the highest r-squared value, with a p -value of 0.00002.

	r^2	p -value
$S_{290-350}$	0.3560	0.00025
$S_{275-295}$	0.4497	0.00002
$S_{350-400}$	0.0443	0.23987
$a_{250}:a_{365}$	0.2645	0.00220
SUVA_{254}	0.1980	0.01376
S_R	0.4540	0.00002

724

725

726 **Figure Legends**

727

728 **Figure 1.** The northern reaches of the Kolyma River in East Siberia and the locations of the 47
729 water samples collected throughout the region in this study (including soil pore waters, streams,
730 rivers, and the Kolyma River mainstem).

731

732 **Figure 2.** Concentrations of (a) dissolved organic carbon (DOC), (b) bioavailable DOC, and (c)
733 percentage of total DOC that is bioavailable for the four water sample types. The mean (hollow
734 squares), median (horizontal lines), ± 1 standard deviation (gray boxes), and total range
735 (whiskers) for each sample population are shown.

736

737 **Figure 3.** Chromophoric dissolved organic carbon (CDOM) absorption spectra from 200–800
738 nm for (a) all samples; and (b) streams, rivers, and the Kolyma River mainstem only.

739

740 **Figure 4.** Relationships between DOC and CDOM absorption at 254, 350, and 440 nm for
741 streams, rivers, and the Kolyma River mainstem.

742

743 **Figure 5.** The six presented CDOM metrics, (a) $S_{290-350}$, (b) $S_{275-295}$, (c) $S_{350-400}$, (d) $a_{250}:a_{365}$, (e)
744 $SUVA_{254}$, and (f) S_R , show the separation between soil pore, stream, river, and Kolyma mainstem
745 waters. The mean (hollow squares), median (horizontal lines), ± 1 standard deviation (gray
746 boxes), and total range (whiskers) for each sample population are shown.

747

748 **Figure 6.** The CDOM metric S_R shows a relatively strong relationship with concentrations of
749 bioavailable DOC present in the sampled waters, with an r-squared value of 0.4540 and p -value
750 <0.01 .

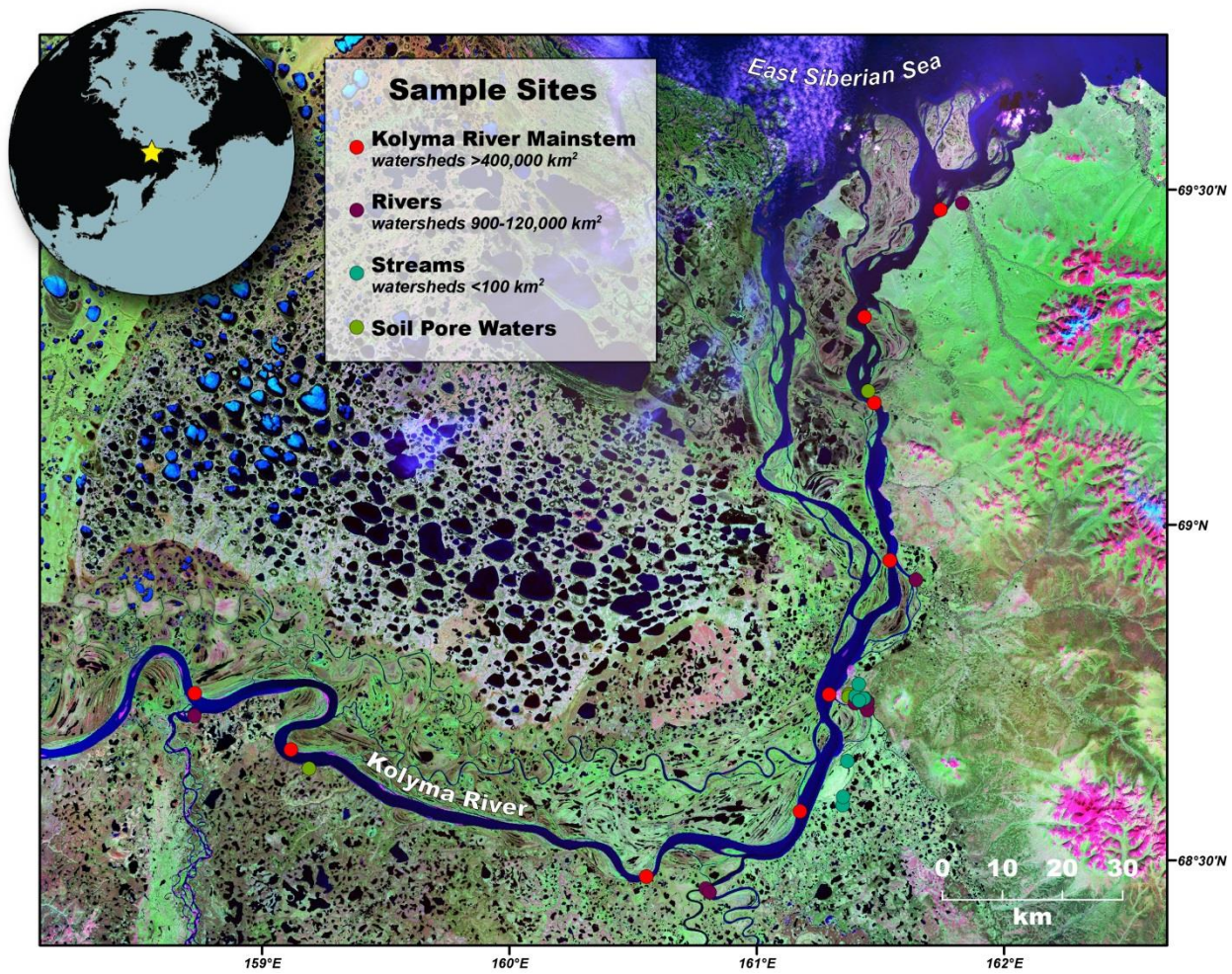


Figure 1.

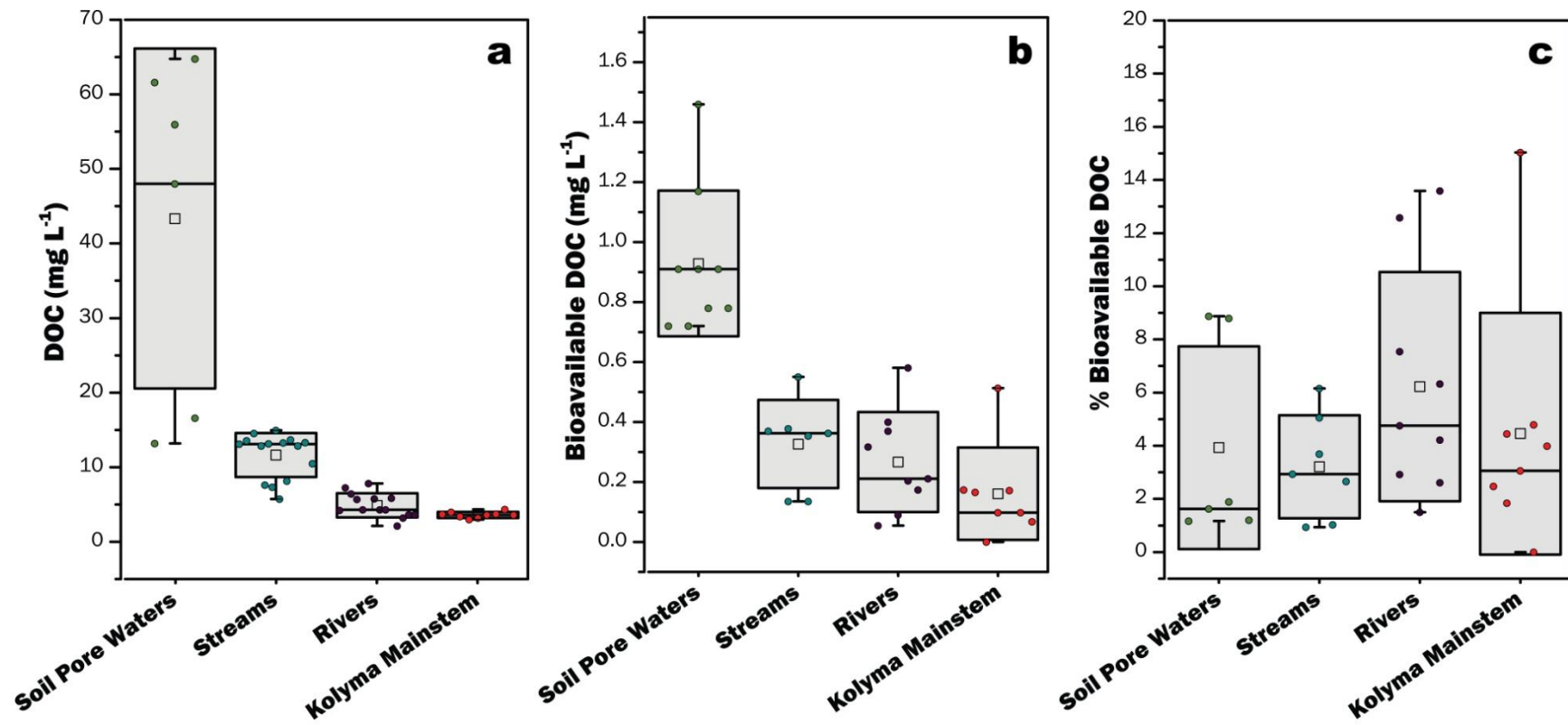


Figure 2.

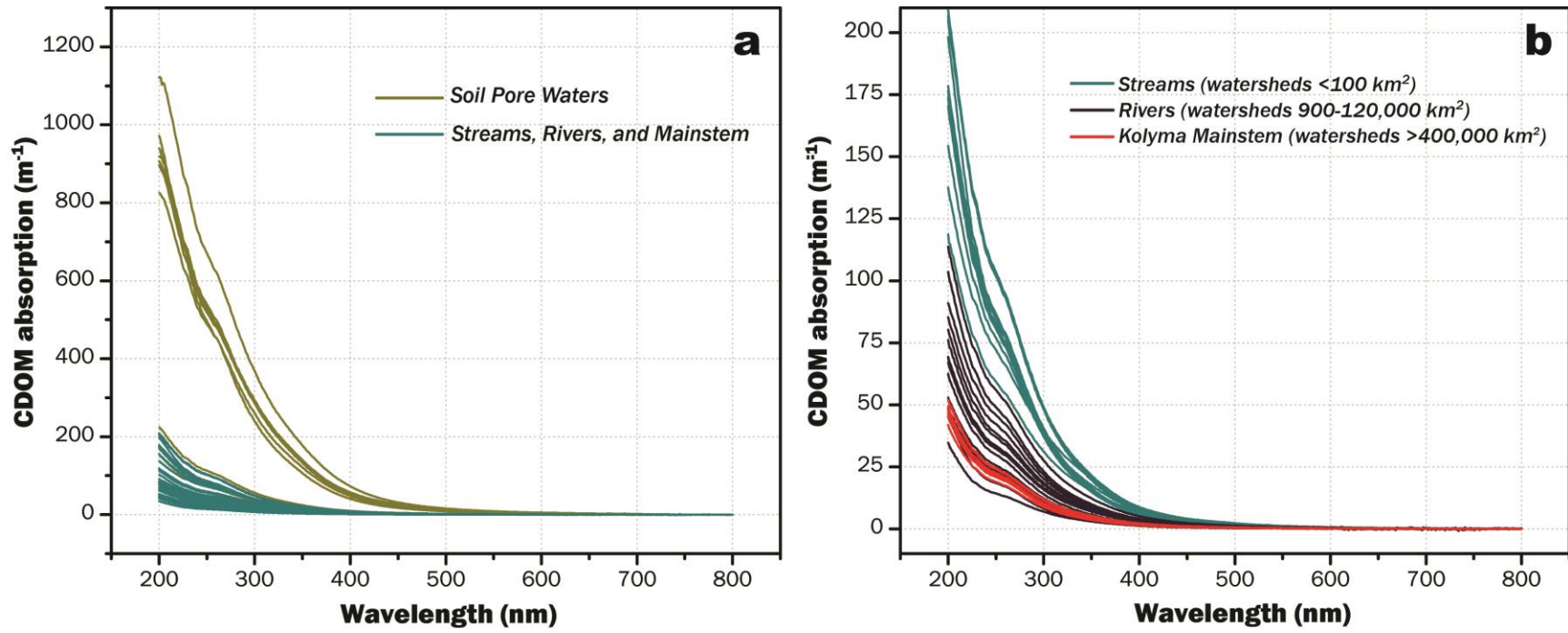


Figure 3.

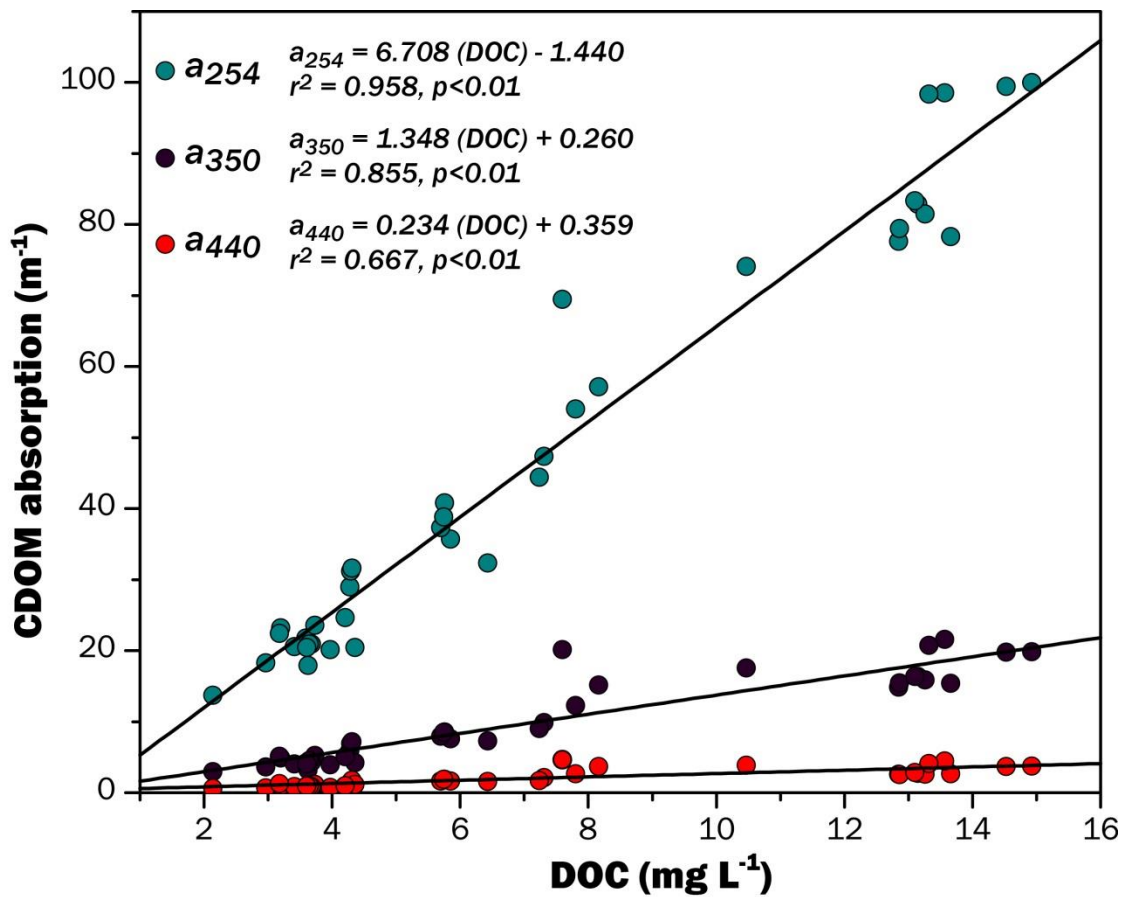


Figure 4.

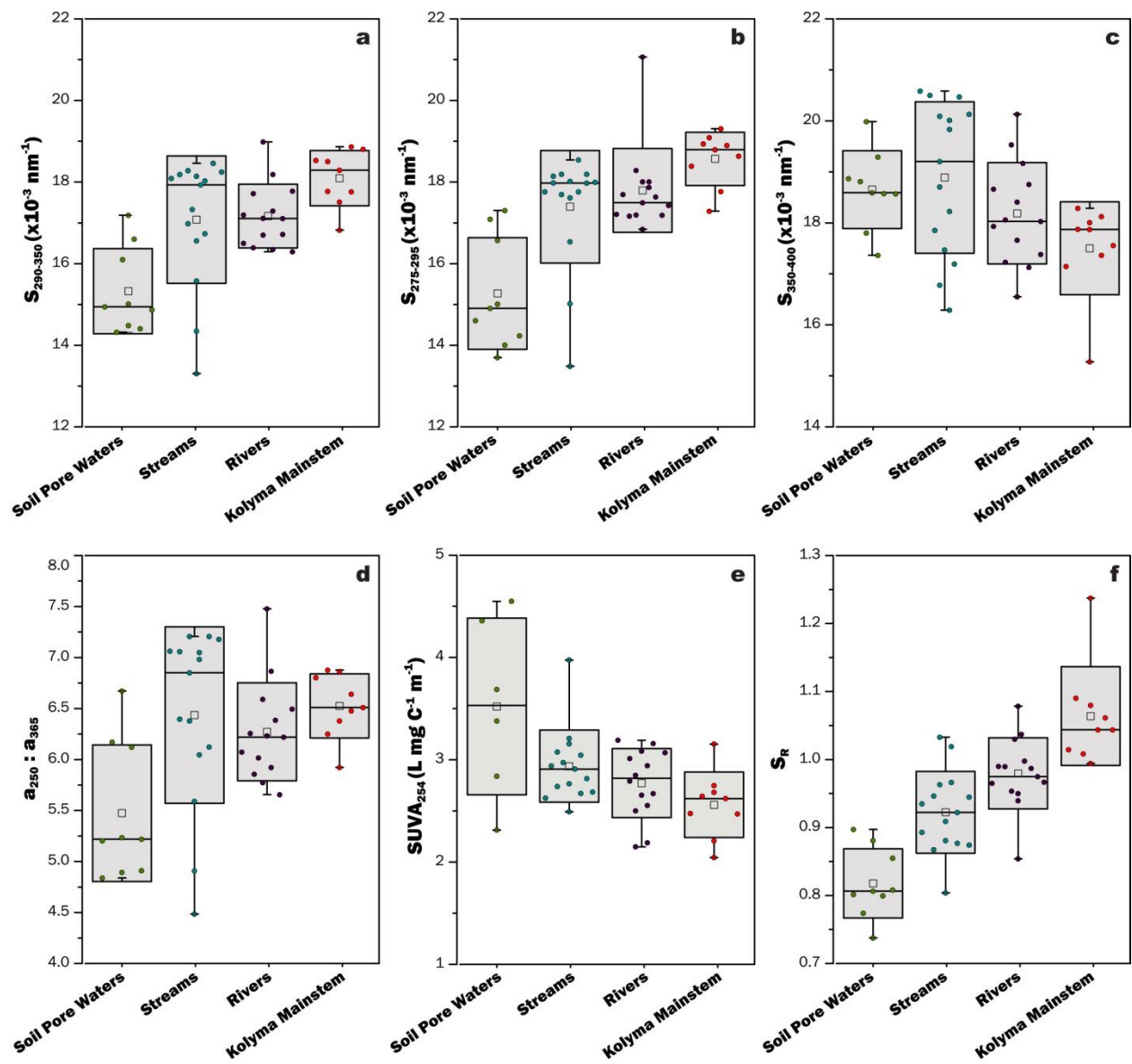


Figure 5.

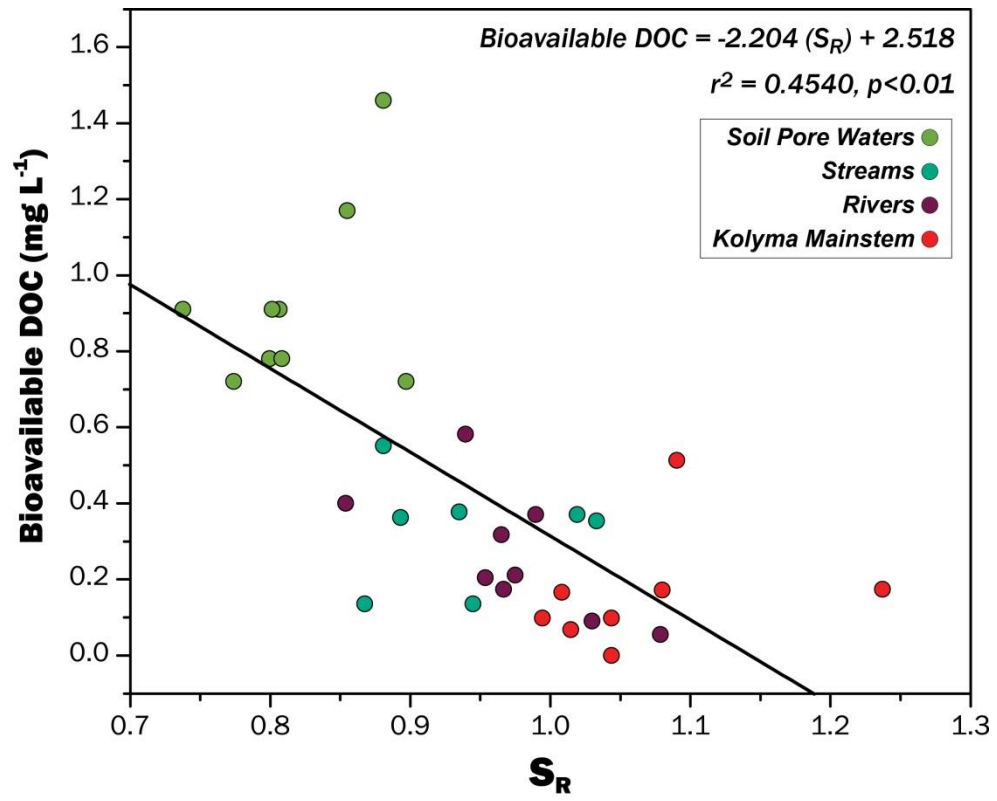


Figure 6.